Carbon Quantum Dot Fluorescent Stickers for Biochip Authentication

Navajit Singh Baban, Mohammed Abdelhameed,
Mahmoud Elbeh, Khalil Ramadi, and Yong-Ak Song
Division of Engg., New York University, Abu Dhabi, UAE.
Email:{nsb359, moa2022, mme7543, kbr5930, rafael.song}@nyu.edu

Sukanta Bhattacharjee
Department of Computer Science and Engineering
Indian Institute of Technology Guwahati, India.
Email: sukantab@iitg.ac.in

Ramesh Karri
Department of Electrical and Computer Engineering
New York University, New York, USA.
Email: rkarri@nyu.edu

Krishnendu Chakrabarty
School of Electrical, Computer and Energy Engineering
Arizona State University, Tempe, AZ, USA.
Email: Krishnendu.Chakrabarty@asu.edu

2024 IEEE 33rd Asian Test Symposium (ATS) | 979-8-3315-2916-1/24/$31.00 ©2024 IEEE | DOI: 10.1109/ATS64447.2024.10915375

***Abstract*—Microfluidic biochips are widely used in biomedical research, clinical diagnostics, and point-of-care testing. However, their complex supply chains make them vulnerable to counterfeiting, overbuilding, and intellectual property (IP) piracy. We present fluorescent carbon quantum dot (CQD) stickers[1] that can be integrated with the polydimethylsiloxane (PDMS) based biochips for authentication. The stickers can be plasma-bonded to biochips made of glass and silicon. A protective spin-coated PDMS layer makes them obscured and tamper-proof. However, they are detectable under UV light and can be authenticated via spectral analysis. The scheme exhibits unique excitation-dependent responses associated with the variability of the CQD sizes. This makes it ideal for physical authentication. Reliability studies concerning mechanical, photonic, and thermal degradation have demonstrated highly stable results. The stability of CQDs within the PDMS, their robust excitation-based emission fluorescence response, and the use of waste polypropylene masks make this a sustainable and robust authenticator for biochips.**

I. Introduction

Microfluidic biochips, a prominent class of lab-on-a-chip devices, integrate biochemical functionalities into a singular miniaturized device, emulating the capabilities of a laboratory [1]. They have revolutionized various domains of biological computing, encompassing enzymatic, deoxyribonucleic acid (DNA), and proteomic analysis, surface immunoassays, toxicity monitoring and point-of-care-testing (POCT) [2].

Biochip companies have embraced horizontal supply-chain models to attain economies of scale and cost reduction [3]. Untrusted third parties in the supply chain present risks of intellectual property (IP) attacks such as reverse engineering [4], counterfeiting [2], overbuilding [1] and, piracy [5]. These issues pose substantial threats, jeopardizing the development of proprietary protocols, diminishing confidence among healthcare professionals in biochips, and adversely affecting patients. The security concerns are emphasized by the inclusion of a medical device cybersecurity provision in the United States' new medical device law [6].

In a separate line of concerns related to plastic recycling, 26,000 metric tons of plastic waste from masks and bags were produced during the COVID-19 period and ended up in the ocean and landfills [7], [8]. Thus, to tackle IP-theft issues while promoting sustainable practices, we introduce a novel authentication scheme using fluorescent watermarking stickers at the biochip device level. The scheme harnesses carbon quantum dots (CQDs) synthesized through a one-step oxidative hydrothermal process from discarded COVID-19 polypropylene masks [7]. We mix CQDs into a polydimethylsiloxane (PDMS) substrate to create fluorescent watermarking stickers. These CQD stickers (CQDS) can be permanently plasma bonded onto biochip devices made of PDMS, glass, or silicon. We refer to these embedded CQDs in the biochip stickers as Bio-CQDS. By spin-coating a layer of PDMS [9], [10] the Bio-CQDS become optically obscured and resistant to tampering as they go subsurface of the spin-coated layer post-curing [11]. However, the obscured Bio-CQDS become identifiable under UV light, and their authentication is accomplished through spectral analysis by correlating the intensity-wavelength response with the database held by the trusted third party (TTP) [12], [11]. Moreover, the Bio-CQDS exhibits an excitation-dependent response due to the variability in CQD sizes [7], which is crucial for generating a broad spectrum of challenge-response pairs for authentication [12]. Furthermore, reliability studies showed that Bio-CQDS exhibited superior mechanical, photonic, and thermal stability compared to fluorescent organic dyes. Scalability studies demonstrated that carbon quantum dots (CQDs) could be efficiently synthesized

[1]For sustainability we derive CQDs from waste polypropylene masks.

979-8-3315-2916-1/24/$31.00 ©2024 IEEE

from polypropylene masks in large quantities with consistent properties, underscoring Bio-CQDS's potential for large-scale production. Additionally, cytotoxicity studies confirmed that CQDs are safe for biochip applications, as they showed minimal impact on cell viability at relevant concentrations, making Bio-CQDS an effective and safe scheme.

The rest of the paper is organized as follows: Section II provides the background, Bio-CQDS threat and authentication model, and prior work. Section III describes the experimental and reliability study results. Sections IV-V present discussions and conclusion, respectively.

II. Background

A. Carbon Quantum Dots

CQDs are zero-dimensional carbon nanomaterials that possess unique physical and chemical properties, low toxicity, easy-to-functionalize surfaces, and good biocompatibility [7]. Further, they are highly soluble in water, alcohol, and various organic solvents, and possess excitation-dependent emission consistent with their size distribution of 1-8 nm [7]. They are extensively used in biological imaging, environmental monitoring, targeted drug delivery, and disease diagnosis [7]. In the context of watermarking applications, CQDs offer great stability within polymer matrices, serving as sustainable and non-toxic alternatives to conventional fluorescent dyes [7]. Their resistance to photobleaching and consistent fluorescence ensure reliable and secure authentication for biochips.

B. Microfluidic Biochips

Microfluidic biochips (MBs) are categorized primarily according to the technologies that drive their functionality, including digital microfluidic biochips (DMFBs) [5], flow-based microfluidic biochips (FMBs) [1], and paper-based microfluidic biochips (PMBs) [13]. Flow-based microfluidic biochips (FMBs) function by steering fluid through microchannel networks etched into substrates like glass or polymers such as PDMS [1]. These biochips precisely and automatically manage nanoliters/picoliters fluid volumes by actuating pressure-driven microvalves made from thin elastomeric membranes [2].

DMFBs utilize electrowetting-on-dielectric (EWOD) to control liquid droplets on an array of electrodes that have a dielectric layer and a superhydrophobic layer [5]. By applying voltage to electrodes, DMFBs adjust the wettability of this dielectric surface, thereby manipulating droplets through changes in surface tension [5]. Paper-based microfluidic biochips (PMBs) leverage capillary action in porous paper for fluid movement without external power, making them suitable for on-site diagnostics and applications in resource-limited areas [13]. PMBs' simplicity, affordability, and compatibility with low-cost detection technologies like colorimetric and electrochemical assays make them attractive for rapid diagnostics in diverse settings, rural to urban [14].

C. Security Threats to Biochips

Untrusted third parties in the biochip supply chain pose risks of IP-theft based attacks including reverse engineering, counterfeiting, overbuilding, and piracy [5]. Below, we present Bio-CQDS threat and authentication model to address the IP-theft threats. Fig. 1 presents the proposed CQDS authentication model of a cyber-physical biochip system, forming a triad that includes the physical biochip embedded with CQDS, a customer, and a trusted third party (TTP). Customers may include research institutions, forensic labs, pharmaceutical and biotech firms, clinical diagnostic centers, hospitals, healthcare services, and retail outlets. The TTP is responsible for authentication, which involves validating authentication response comprising Bio-CQDS spectral scan data.

We assume that the customer is equipped with a spectrometer for recording the spectral response of Bio-CQDS, and the TTP can authenticate the Bio-CQDS by matching the response present in its database. The customer is responsible for sending the Bio-CQDS spectral emission response to the TTP for provenance authentication. In the threat model, the attacker aims to replace a genuine Bio-CQDS with a counterfeit one while still passing authentication with the TTP. However, the spectral response of a Bio-CQDS, which is determined by the size distribution of CQDs, is a unique property that is extremely unlikely for an attacker to replicate or counterfeit, making the authentication scheme robust.

D. Prior Work on Biochip Security

Previous efforts to safeguard biochips from IP-theft attacks have centered around watermarks [1], molecular barcodes [15], bioassay locking [16] and obfuscation [5], [17]. Liang et al. employed molecular barcodes at the protocol level to fortify the protection of biochemical sample intellectual property [15]. This hierarchical approach involved the incorporation of secret signatures through variables like mixing ratio, incubation time, and sensor calibration to safeguard the bio-sample integrity.

Baban et al. introduced a watermarking scheme for FMBs by changing the height of micro reaction chambers or microchannels at specific positions, thereby creating discernible fluorescent watermarks that could be quantified using fluorescence microscopy [1]. In a recent work, Baban et al.

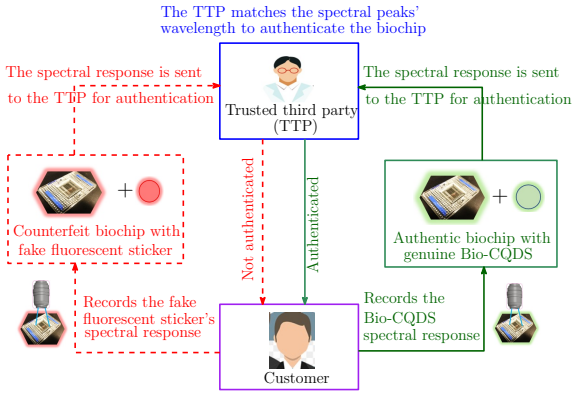

Fig. 1. Bio-CQDS threat and authentication model: The solid green lines depict successful authentication by the TTP for an authentic biochip with a genuine Bio-CQDS. The red dashed lines depict unsuccessful authentication by the TTP for a counterfeit biochip with a fake Bio-CQDS.

introduced a dynamic material-level watermarking scheme for PDMS-based FMBs utilizing a perylene-labeled fluorescent organic dye [2]. Recently, Baban et al. reported an image-based PUF (Biochip-PUF) [12] based on the inherent stochasticity of the biaxial response of the microvalves that varied from valve to valve. Thus far, the potential of CQD infused watermarking stickers for IP-theft protection in biochips has not been fully explored, despite their benefits such as stability, bio-compatibility, high quantum yield, and tunable emission properties [7].

III. CQD-based Authentication of Biochips

A. Fluorescence and Spectral Response of Bio-CQDS

CQD-infused PDMS samples were prepared with a 10:1 weight ratio, where 10 parts were PDMS (SYLGARD 184 silicone elastomer) with the curing agent and one part was the CQD solution in Tetrahydrofuran (THF). Optical assessments were carried out on American Society for Testing and Materials (ASTM) D412 Type C [9], [10] dog-bone-shaped control (10:0) and CQD-infused (10:1) PDMS samples. The control and CQD-infused PDMS samples were observed under both visible light and UV irradiation (365 nm). When subjected to UV light, the CQD-infused sample exhibited fluorescence, whereas the control sample displayed no fluorescence. Furthermore, we conducted an investigation into the CQD distribution within the PDMS film via confocal microscopy using 470 nm excitation. This analysis revealed a uniform dispersal of CQDs throughout the PDMS matrix, ensuring consistency.

We utilized a 4 mm biopsy punch to create fluorescent circular stickers from the CQD-infused PDMS samples. Subsequently, these stickers were permanently affixed to a laboratory-made biochip using plasma bonding [9], [18], thus making them Bio-CQDS. Plasma bonding is a technique that permanently bonds PDMS to materials such as glass and silicon by treating the surfaces with plasma, typically oxygen or air [19]. To render Bio-CQDS obscured and tamper-proof, a layer of PDMS was spin-coated at 750 rpm for 30 seconds on top of it, after which it was cured. This process rendered the Bio-CQDS obscured under visible light and tamper-proof via placing it subsurface permanently bonded with the bottom and vicinal PDMS, as seen in Fig. 2(a). The obscured sticker can be illuminated and identified using UV light, as seen in Fig. 2(b). Next, the process includes matching the excitation-dependent emission spectral response with the database records of the Trusted Third Party (TTP) for Bio-CQDS authentication.

Fig. 2(c) shows the spectral response of excitation-dependent emission, employing three distinct excitation wavelengths (405 nm, 488 nm, and 514 nm). The response revealed distinct emission peaks at different excitation wavelengths (510 nm, 570 nm, and 590 nm), exhibiting highly consistent outcomes across triplicate measurements (three sticker samples replicated from a single batch). Fig. 2(d) shows a comparison of emission peaks from two batches of CQDS, synthesized from different COVID-19 waste polypropylene masks, at excitation wavelengths of 405 nm, 488 nm, and 514 nm. The graph recorded variances of 13% at 405 nm, 4% at 488 nm, and only 2% at 514 nm between the batches, suggesting a relatively consistent synthesis process with minor batch-to-batch variability. The variation can be ascribed to the distinct polypropylene compositions stemming from various manufacturers' masks. Consequently, TTP requires that each CQD batch be documented separately to ensure accurate authentication.

Fig. 2(e) shows more excitation-dependent emission response pairs, highlighting a wide range of Bio-CQDS authentication parameters. Additionally, the variance in distances between emission peaks at different excitation wavelengths contributes to a broader set of authentication parameters, thereby enhancing the robustness of validation. This excitation-dependent emission is due to the variability in the size of CQDs [7]. Fig. 2(f) displays a transmission electron microscopy (TEM) image and size distribution histograms of CQDs, which are quasi-spherical in shape with no noticeable aggregation or agglomeration. The average diameter of the CQDs is recorded at 4.52 nm. Thus, the spectral response of Bio-CQDS is attributed to the size distribution of CQDs, unlike fluorescent organic dyes with uniform molecular sizes. This tunable and size-dependent nature of quantum dots provides a more diverse spectral response and enhances security features for biochip authentication, surpassing traditional organic dyes.

B. Mechanical Characterization of PDMS Samples with CQD

To evaluate how CQD affects the mechanical behavior of PDMS, we performed mechanical characterization of the control (PDMS only) and CQD-mixed PDMS samples (ASTM D412 C) [10] with different concentrations. The experimental setup is shown in Fig. 3(a), where a 5 mm/s displacement rate was used for characterization. The load cell used for force measurement had a capacity of 5 kN. The results in Fig. 3(b) and Fig. 3(c) illustrate that there is no significant difference in the stiffness of the PDMS samples when CQDs are mixed. Fig. 3(d) shows the stress-strain response, where the modulus of the CQD-infused PDMS (10:1) was recorded to be 1.2 MPa, which is consistent with the PDMS modulus without any CQD infusion, as evident from the stiffness plot. Figs. 3(e-h) show the hysteresis strain energy response for the control and CQD-infused PDMS samples with three different concentrations. The samples were subjected to 5 cycles of cyclic deformation at a 5 mm/s displacement rate. The results indicate a comparable hysteresis strain energy response between the control and the CQD mixed samples with different concentrations. Thus, adding CQDs in PDMS did not affect the mechanical behavior of the PDMS samples.

C. Reliability Studies

Under ambient air condition, we tested the photostability of Bio-CQDS by exposing them to UV illumination from a 250 W mercury lamp, which delivers power 134 times greater than the 1.86 W of ambient lighting. We monitored the fluorescence response at a 405 nm excitation wavelength at various times

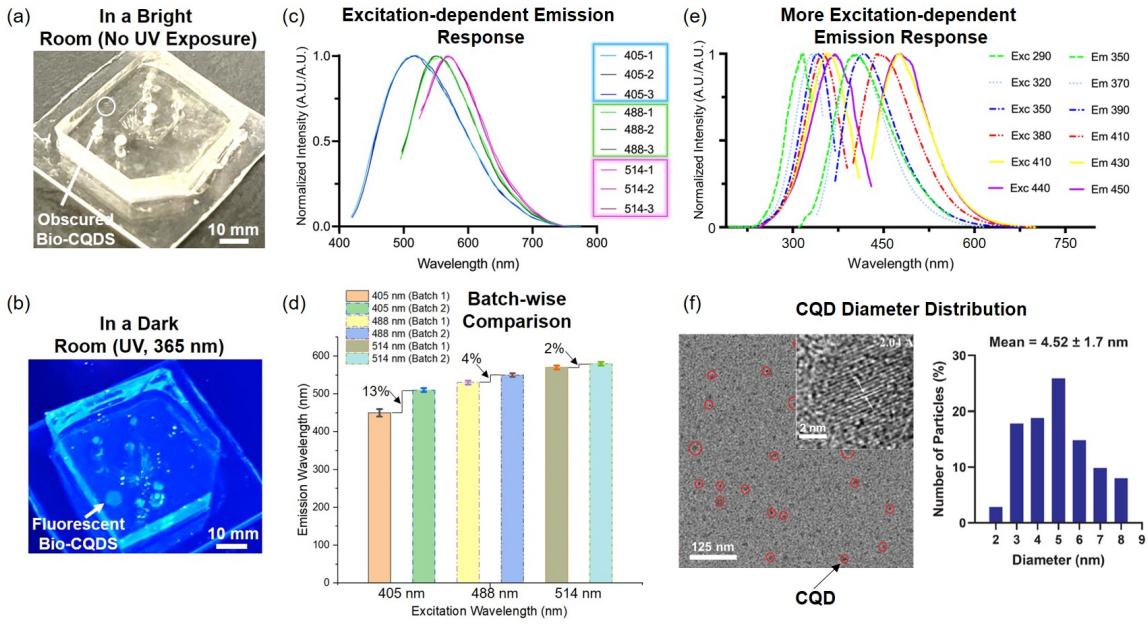

Fig. 2. Obscuring Bio-CQDS via spin coating and spectral Response: (a) Bio-CQDS remains obscured under visible light due to a spin-coated PDMS layer (750 rpm for 30s), which also renders it tamper-proof. (b) Bio-CQDS is visible under UV light (365 nm), especially in a dark room. (c) Excitation-dependent spectral response using confocal microscopy atexcitation wavelengths of 405 nm, 488 nm, and 514 nm. The response shows emission peaks for different excitation wavelengths. Normalization of the intensity was done using the maximum value. (d) Comparison of emission peaks between two Bio-CQDS batches synthesized from two different COVID-19 waste polypropylene mask samples. The number of samples tested was five, and the error bar depicts the standard deviation. (e) Excitation-dependent spectral response of Bio-CQDS at more wavelengths, highlighting a wide range of authentication parameters. (f) The excitation-dependent emission response is due to CQD size variability. The figure shows CQD diameter distribution. The mean diameter recorded is 4.52 nm.

ranging from 1 to 24 hours. The results shown in Fig. 4(a) indicate that the fluorescence intensity reduced by 25% and 43% when continuously irradiated for 12 hours and 24 hours, respectively. Although the 43% reduction in the intensity appears significant, it is important to consider the high power of the illumination (250 W), which suggests that the CQDs exhibit considerable stability. Notably, no shift in the emission wavelength was observed, which was 510 nm (see Fig. 2(c)). Despite reduced intensity, the CQDS can still authenticate due to the stable emission peak, the key authentication parameter.

To assess the thermal stability, CQDS were excited at 405 nm for 24 hours, and we recorded the fluorescent intensity and any emission wavelength spectral shifts from 20°C to 100°C. The findings, shown in Fig. 4(b), indicate that there is a reduction in fluorescence intensity of 10% at 60°C and 23% at 100°C, with no emission wavelength shift, affirming the thermal stability of CQDS within the tested temperature spectrum.

We investigated the mechanical behavior of control and CQD-infused PDMS samples over a one-year period. The results, depicted in Fig. 4(c), showed a slight decrease in stiffness, with an 8% reduction for PDMS only and a 5% reduction for PDMS with CQDs. Additionally, there was a slight increase in hysteresis strain energy, with a 9% rise for PDMS only and 3% for PDMS with CQDs, as can be seen in Fig. 4(d). These modest changes can be ascribed to the inherent aging effects of PDMS, as observed in the control samples [20], [21]. The infusion of CQDs, therefore, did not significantly alter the natural aging of PDMS, maintaining stable mechanical properties throughout the period.

Bio-CQDS mechanical stability is vital for authentication, given their embedding in deformable PDMS prone to biochip-induced or tampering-related deformation. Our year-long investigation into the mechanical behavior of control and CQD-infused PDMS samples revealed only minor changes in stiffness and hysteresis strain energy, primarily due to the natural aging of PDMS. Consequently, the stable mechanical properties effectively counter any functional or deliberate deformation-based tampering, ensuring that Bio-CQDS reliably fulfills its authentication role with minimal impact from aging.

IV. Discussions and Additional Results

Bio-CQDS is a novel authentication scheme that leverages the excitation-dependent emission characteristics of CQDs, which arise from the nano-level size variability of the quantum dots, a feature absent in organic dyes that are molecule-based and have only one size [22], [23]. Furthermore, the spectral response of Bio-CQDS can be diversified by adjusting parameters such as concentration, size distribution, acid concentration, reaction time, and temperature, enhancing authentication flexibility [7]. Moreover, instead of placing just one Bio-CQDS sticker, multiple stickers with variable CQD distributions can be placed onto the chip, and randomized checkpointing can be used for a stronger authentication protocol [5], [24].

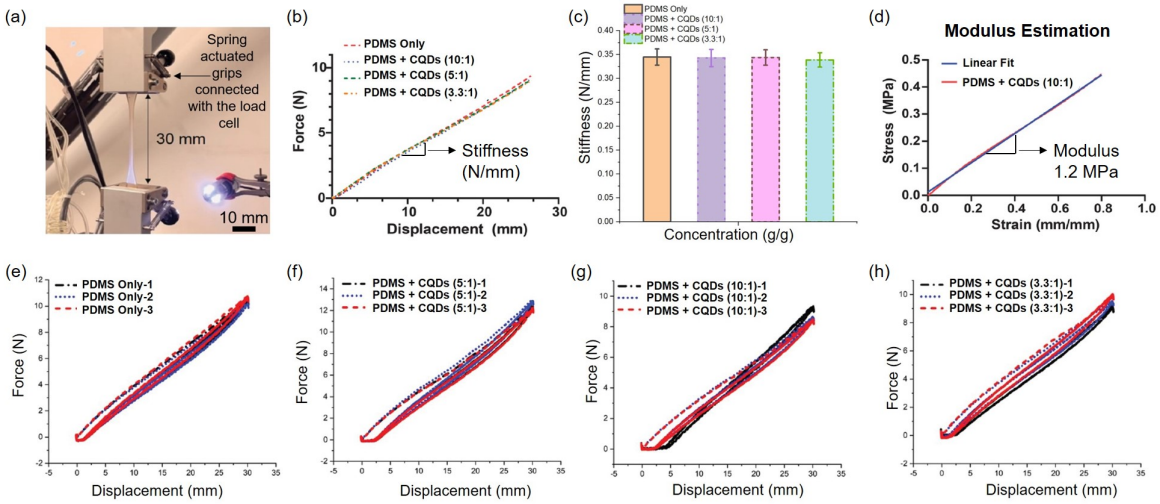

Fig. 3. Mechanical characterization of CQD-infused ASTM D412 C PDMS samples: (a) Experimental setup showing the displacement-controlled deformation of the PDMS sample connected to the load cell via spring-actuated grips. (b) Force-displacement responses for the control and samples with different CQD concentrations. The slope of the linear curve gives the stiffness value. (c) Comparison of stiffness across the control sample and the samples with different concentrations. The number of samples is five, and the error plot shows the standard deviation. (d) Stress-strain response of the CQD-infused PDMS (10:1) sample with a Young's modulus of elasticity of 1.2 MPa. (e) Hysteresis strain energy response of the control (PDMS only) samples. (f) Hysteresis strain energy response of the CQD-infused PDMS (10:1) samples. (g) Hysteresis strain energy response of the CQD-infused PDMS (5:1) samples. (h) Hysteresis strain energy response of the CQD-infused PDMS (3.3:1) samples.

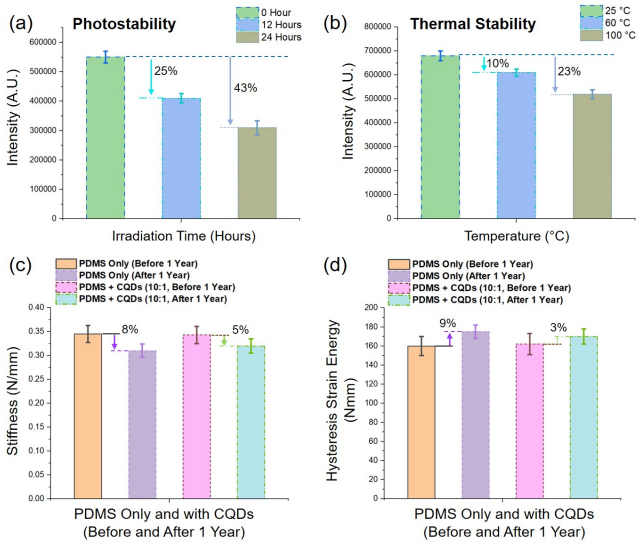

Fig. 4. Stability test results: (a) Photostability results. (b) Thermal stability results. (c) Stiffness comparison of CQD-infused PDMS samples post one year. (d) Hysteresis strain energy comparison of CQD-infused PDMS samples post one year. Five samples were tested and the error bar indicates standard deviation.

The ability of Bio-CQDS to permanently bond with glass, PDMS, and silicon through plasma bonding makes it as an effective choice for creating mechanically robust and tamper-proof embedded watermarking stickers. Unlike traditional adhesive-based methods such as electronic radio-frequency identification (RFID) tags, depth holograms, and barcode or quick-response (QR) code stickers, which are prone to replication and tampering, Bio-CQDS offers a more secure and durable alternative for authentication purposes [25].

Traditional technologies such as scanning electron microscopy (SEM) for material composition analysis are reliable but destructive and limited to individual sample testing, making them impractical for widespread use [25]. Nondestructive techniques such as X-Ray fluorescence (XRF) and Energy Dispersive X-Ray Spectroscopy provide insights into material composition and potential tampering but are complex, time-consuming, and require expertise, challenging for industries with extensive supply chains [25]. In contrast, Bio-CQDS offers a simpler, nondestructive authentication solution, suitable for large-scale operations without much experties.

Reliability studies, examining photo-, thermal-, and mechanical-stability, demonstrated that Bio-CQDS are highly stable within a PDMS matrix. The inherent stability of CQDs is attributed to their carbon-based core, surface functionalization, size, and quantum confinement effects, making them resistant to photobleaching, thermal degradation, and chemical reactions [26], [27]. For CQDs, we conducted a scalability study where we synthesized carbon quantum dots (CQDs) from polypropylene masks using hydrothermal reactions with varying mask loads (0.5, 1, 1.5 g) in an autoclave reactor [7]. The increase in mask load led to higher fluorescence intensity due to the formation of more carbon dots. Additionally, by adjusting the mask loads (1, 2 g) and the volume of the nitric acid solution (20 ml, 40 ml), we successfully scaled up the synthesis process, producing carbon dots with consistent properties in a larger reactor (100 ml, 200 ml) [7]. We recorded that this process is scalable up to 7.5% of the mask waste load, indicating the potential for large-scale production of CQDs from polypropylene masks [7].

Cytotoxicity refers to the property of being toxic to cells.

It can be caused by various agents such as toxic chemicals, radiation, and certain venoms [28]. To evaluate the cytotoxicity of carbon quantum dots (CQDs), we conducted an MTT assay on HeLa cells using varying concentrations of CQDs (0, 0.1, 0.25, 0.5, 1, and 2 mg/ml) and assessed cell viability after 4 and 24 hours [7]. The results indicated minimal impact on cell viability at concentrations up to 1 mg/ml for 4 hours and up to 0.5 mg/ml for 24 hours. However, cell viability decreased to approximately 55% and 45% at higher concentrations (2 mg/ml for 4 hours and 1 mg/ml for 24 hours, respectively). These findings suggest that CQDs at a concentration of 0.5 mg/ml do not significantly affect cell viability, supporting their potential for use in Bio-CQDS embedded in the biochip portion that comes into contact with sample fluids containing cells or other biomolecules.

V. Conclusion

We developed Bio-CQDS: fluorescent PDMS watermarking stickers containing carbon quantum dots (CQDs) derived from waste polypropylene masks to counter IP-theft threats on biochips. These stickers, plasmabonded to PDMS, glass, or silicon biochip devices, are shielded by a spin-coated PDMS layer for tamper-proofing. Visible under UV light, Bio-CQDS can be authenticated using spectral analysis, with excitation-dependent responses yielding diverse parameters. Stability tests show CQDs within the PDMS matrix are mechanically, photonic, and thermally stable. Scalable production from masks ensures consistent properties, and cytotoxicity studies confirm safety, making Bio-CQDS a sustainable, robust authentication solution for biochips.

VI. Acknowledgment

We thank the National Science Foundation (NSF) for funding support. Karri was supported in part by NSF award 2049311, and Chakrabarty in part by NSF grant 2049335.

References

[1] N. S. Baban, S. Saha, A. Orozaliev, J. Kim, S. Bhattacharjee, Y. Song, R. Karri, and K. Chakrabarty, "Structural attacks and defenses for flow-based microfluidic biochips," *IEEE Transactions on Biomedical Circuits and Systems.*, vol. 16, no. 6, pp. 1261–1275, 2022.

[2] N. S. Baban, S. Saha, S. Jancheska, I. Singh, S. Khapli, M. Khobdabayev, J. Kim, S. Bhattacharjee, Y.-A. Song, K. Chakrabarty *et al.*, "Material-level countermeasures for securing microfluidic biochips," *Lab on a Chip*, vol. 23, no. 19, pp. 4213–4231, 2023.

[3] S. S. Ali, M. Ibrahim, J. Rajendran, O. Sinanoglu, and K. Chakrabarty, "Supply-chain security of digital microfluidic biochips," *Computer*, vol. 49, no. 8, pp. 36–43, 2016.

[4] H. Chen, S. Potluri, and F. Koushanfar, "Biochipwork: Reverse engineering of microfluidic biochips," in *IEEE International Conference on Computer Design*, 2017, pp. 9–16.

[5] S. Mohammed, S. Bhattacharjee, Y.-A. Song, K. Chakrabarty, and R. Karri, *Security of Biochip Cyberphysical Systems*. Springer, 2022.

[6] "Exclusive: FDA leader on impact of new medical device law," 2023. [Online]. Available: https://www.bankinfosecurity.com/interviews/exclusive-fdas-device-cyber-leader-on-new-laws-impact-i-5216

[7] M. Abdelhameed, M. Elbeh, N. S. Baban, L. Pereira, J. Matula, Y.-A. Song, and K. B. Ramadi, "High-yield, one-pot upcycling of polyethylene and polypropylene waste into blue-emissive carbon dots," *Green Chemistry*, vol. 25, no. 5, pp. 1925–1937, 2023.

[8] A. E. Ongaro, Z. Ndlovu, E. Sollier, C. Otieno, P. Ondoa, A. Street, and M. Kersaudy-Kerhoas, "Engineering a sustainable future for point-of-care diagnostics and single-use microfluidic devices," *Lab on a Chip*, vol. 22, no. 17, pp. 3122–3137, 2022.

[9] N. S. Baban, A. Orozaliev, S. Kirchhof, C. J. Stubbs, and Y.-A. Song, "Biomimetic fracture model of lizard tail autotomy," *Science*, vol. 375, no. 6582, pp. 770–774, 2022.

[10] N. S. Baban, A. Orozaliev, C. J. Stubbs, and Y. A. Song, "Understanding interfacial fracture behavior between microinterlocked soft layers using physics-based cohesive zone modeling," *Physical Review E*, vol. 102, no. 1, pp. 012 801–012 820, 2020.

[11] N. S. Baban, S. Saha, S. Jancheska, J. Zhou, S. Vijayavenkataraman, S. Bhattacharjee, Y.-A. Song, K. Chakrabarty, and R. Karri, "Bio-FP: Biochip fingerprints for authentication," in *IEEE Biomedical Circuits and Systems Conference*, 2023, pp. 1–5.

[12] N. S. Baban, A. Orozaliev, Y.-A. Song, U. Chatterjee, S. Bose, S. Bhattacharjee, R. Karri, and K. Chakrabarty, "Biochip-PUF: Physically unclonable function for microfluidic biochips," in *IEEE International Test Conference*, 2023, pp. 166–175.

[13] S. Kummari, L. R. Panicker, J. Rao Bommi, S. Karingula, V. Sunil Kumar, K. Mahato, and K. Y. Goud, "Trends in paper-based sensing devices for clinical and environmental monitoring," *Biosensors*, vol. 13, no. 4, pp. 420–451, 2023.

[14] S. H. Baek, C. Park, J. Jeon, and S. Park, "Three-dimensional paper-based microfluidic analysis device for simultaneous detection of multiple biomarkers with a smartphone," *Biosensors*, vol. 10, no. 11, pp. 187–199, 2020.

[15] T.-C. Liang, K. Chakrabarty, T. Abaffy, H. Matsunami, and R. Karri, "Securing biochemical samples using molecular barcoding on digital microfluidic biochips," in *IEEE Biomedical Circuits and Systems Conference*, 2021, pp. 01–06.

[16] S. Bhattacharjee, J. Tang, S. Poddar, M. Ibrahim, R. Karri, and K. Chakrabarty, "Bio-chemical assay locking to thwart bio-ip theft," *ACM Transactions on Design Automation of Electronic Systems*, vol. 25, no. 1, pp. 5:1–5:20, 2020.

[17] M. Shayan, S. Bhattacharjee, A. Orozaliev, Y.-A. Song, K. Chakrabarty, and R. Karri, "Thwarting Bio-IP theft through dummy-valve-based obfuscation," *IEEE Transactions on Information Forensics and Security*, vol. 16, pp. 2076–2089, 2020.

[18] N. S. Baban, A. Orozaliev, C. J. Stubbs, and Y.-A. Song, "Biomimicking interfacial fracture behavior of lizard tail autotomy with soft microinterlocking structures," *Bioinspiration & Biomimetics*, vol. 17, no. 3, p. 036002, 2022.

[19] A. Borók, K. Laboda, and A. Bonyár, "PDMS bonding technologies for microfluidic applications: A review," *Biosensors*, vol. 11, no. 8, pp. 292–320, 2021.

[20] Z. Brounstein, J. Zhao, D. Geller, N. Gupta, and A. Labouriau, "Long-term thermal aging of modified sylgard 184 formulations," *Polymers*, vol. 13, no. 18, pp. 3125–3149, 2021.

[21] I. D. Johnston, D. K. McCluskey, C. K. Tan, and M. C. Tracey, "Mechanical characterization of bulk sylgard 184 for microfluidics and microengineering," *Journal of Micromechanics and Microengineering*, vol. 24, no. 3, pp. 035 017–035 025, 2014.

[22] M. G. Giordano, G. Seganti, M. Bartoli, and A. Tagliaferro, "An overview on carbon quantum dots optical and chemical features," *Molecules*, vol. 28, no. 6, pp. 2772–2790, 2023.

[23] M. Pirsaheb, A. Asadi, M. Sillanpää, and N. Farhadian, "Application of carbon quantum dots to increase the activity of conventional photocatalysts: A systematic review," *Journal of Molecular Liquids*, vol. 271, pp. 857–871, 2018.

[24] J. Tang, M. Ibrahim, K. Chakrabarty, and R. Karri, "Secure randomized checkpointing for digital microfluidic biochips," *IEEE Transactions on Computer-Aided Design of Integrated Circuits and Systems*, vol. 37, no. 6, pp. 1119–1132, 2017.

[25] T. Kulkarni, N. Chawla, and G. Subbarayan, "Physical authentication of electronic devices using synthetically generated 3d material signatures," in *IEEE Electronic Components and Technology Conference*, 2023, pp. 955–959.

[26] Y. Wang and A. Hu, "Carbon quantum dots: synthesis, properties and applications," *Journal of Materials Chemistry C*, vol. 2, no. 34, pp. 6921–6939, 2014.

[27] R. Das, R. Bandyopadhyay, and P. Pramanik, "Carbon quantum dots from natural resource: A review," *Materials Today Chemistry*, vol. 8, pp. 96–109, 2018.

[28] I. Canga, P. Vita, A. I. Oliveira, M. Á. Castro, and C. Pinho, "In vitro cytotoxic activity of african plants: A review," *Molecules*, vol. 27, no. 15, pp. 4989–5007, 2022.